



Climatic dynamics and topography control genetic variation in Atlantic Forest montane birds



Gregory Thom^{a,b,*}, Brian Tilston Smith^b, Marcelo Gehara^{c,d}, Júlia Montesanti^e,
Matheus S. Lima-Ribeiro^f, Vitor Q. Piacentini^g, Cristina Y. Miyaki^a, Fabio Raposo do Amaral^e

^a Departamento de Genética e Biologia Evolutiva, Universidade de São Paulo, Rua do Matão, 277, Cidade Universitária, São Paulo, SP 05508-090, Brazil

^b Department of Ornithology, American Museum of Natural History, NY 10024, USA

^c Sackler Institute for Comparative Genomics, American Museum of Natural History, NY 10024, USA

^d Department of Biological Sciences, Rutgers University, 195 University Ave, Newark, NJ 07102, USA

^e Departamento de Ecologia e Biologia Evolutiva, Universidade Federal de São Paulo. Rua Prof. Artur Riedel, 275, Jardim Eldorado, Diadema, SP CEP 09972-270, Brazil

^f Laboratório de Macroecologia, Universidade Federal de Goiás, Jataí, GO, Brazil

^g Departamento de Biologia e Zoologia, Instituto de Biociências, Universidade Federal de Mato Grosso, Cuiabá, Brazil

ARTICLE INFO

Keywords:

Population genomics
Biodiversity hotspot
Endemic species
Historical demography

ABSTRACT

Montane organisms responded to Quaternary climate change by tracking suitable habitat along elevational gradients. However, it is unclear whether these past climatic dynamics generated predictable patterns of genetic diversity in co-occurring montane taxa. To test if the genetic variation is associated with historical changes in the elevational distribution of montane habitats, we integrated paleoclimatic data and a model selection approach for testing the demographic history of five co-distributed bird species occurring in the southern Atlantic Forest sky islands. We found that changes in historical population sizes and current genetic diversity are attributable to habitat dynamics among time periods and the current elevational distribution of populations. Taxa with populations restricted to the more climatically dynamic southern mountain block (SMB) had, on average, a six-fold demographic expansion, whereas the populations from the northern mountain block (NMB) remained constant. In the current configuration of the southern Atlantic Forest montane habitats, populations in the SMB have more widespread elevational distributions, occur at lower elevations, and harbor higher levels of genetic diversity than NMB populations. Despite the apparent coupling of demographic and climatic oscillations, our data rejected simultaneous population structuring due to historical habitat fragmentation. Demographic modeling indicated that the species had different modes of differentiation, and varied in the timing of divergence and the degree of gene flow across mountain blocks. Our results suggest that the heterogeneous distribution of genetic variation in birds of the Atlantic Forest sky islands is associated with the interplay between topography and climate of distinct mountains, leading to predictable patterns of genetic diversity.

1. Introduction

Pleistocene climatic oscillations shaped the genetic diversity and geographical distributions of taxa (Carnaval et al., 2009; Cheng et al., 2013; Colinvaux et al., 1997; Hewitt, 2004; Oswald and Steadman, 2015). The impacts of climatic cycles were particularly acute in sky islands, where montane habitats are fragmented by valleys with drastic environmental differences (Amaral et al., 2018; Graham et al., 2014; Janzen, 1967; McCormack et al., 2009; Mutke et al., 2014; Pie et al., 2018). In montane regions, species respond to climate by changing their ranges in elevation (Chen et al., 2009; Flantua et al., 2019; Freeman et al., 2018; Moritz et al., 2008). During warmer interglacial periods,

cold-adapted species track habitats upslope, producing the fragmented and isolated distributions currently observed in many montane taxa (Flantua et al., 2019). In contrast, during colder glacial periods, species distributions tend to shift downslope, increasing spatial connectivity (DeForest Safford, 1999; Ramírez-Barahona and Eguiarte, 2013). While it is understood that many organisms track habitat in response to climatic oscillations, it is less clear how the physical features of mountains interact with genetic drift and shape the predictability of demographic history. Modeling patterns of genetic variation, population structuring, and gene flow regimes in sky-island systems will help clarify how diversity arises in species-rich montane environments (Badgley et al., 2017).

* Corresponding author.

E-mail address: gthomesilva@amnh.org (G. Thom).

<https://doi.org/10.1016/j.ympev.2020.106812>

Received 16 October 2019; Received in revised form 17 February 2020; Accepted 25 March 2020

Available online 04 April 2020

1055-7903/ © 2020 Elsevier Inc. All rights reserved.

The climatic stratification of elevational gradients produces strong associations of montane organisms to narrow elevational ranges, especially in the tropics where seasonality is less pronounced (Cadena et al., 2012; Janzen, 1967; Kozak and Wiens, 2007). Multiple lines of evidence support that the historical habitat dynamics of a mountain range may be a good predictor of the genetic diversity of elevation-limited taxa. For example, populations restricted to the tops of mountains have a high probability of undergoing bottlenecks and local extirpation as temperatures increase (Freeman and Class Freeman, 2014; La Sorte and Jetz, 2010; Laurance et al., 2011; Şekercioglu et al., 2012; Sorte et al., 2014). In contrast, populations distributed in the foothills may expand geographically, if the surface area of the mountain is higher in mid elevations (Elsen and Tingley, 2015; Freeman et al., 2018). Similarly, habitats at the tops of mountains, which have smaller areas, are expected to be more readily fragmented under changing climates than those distributed at lower elevations (Hewitt, 2004). If the elevational distribution of populations controls genetic diversity, then co-occurring populations should harbor similar levels of variation. Alternatively, if genetic diversity is decoupled from elevational distributions, then co-occurring species should exhibit varying levels of genetic variation. In the latter scenario, historical contingencies associated with independent species histories and differing selective regimes may dictate patterns of standing genetic variation.

To explore the effects of climate-mediated population dynamics of co-occurring taxa, we focus on the southern Atlantic Forest (hereafter AF) sky-island system, located in the coastal region of Brazil. The montane regions of the southern AF are characterized by microclimates associated with specific elevational ranges, which are generally distributed in patches given the high roughness of the relief (Alves et al., 2010; DeForest Safford, 1999; Eisenlohr et al., 2013). Palynological data indicate very dynamic environments in the last 130,000 ya, with more widespread subtropical habitats during colder climatic periods (Behling et al., 2007; Behling and Pillar, 2007; Behling and Safford, 2010; de Oliveira et al., 2012; Flantua et al., 2015; Ledru et al., 2009). The southern AF is composed of distinct mountain ranges that are not continuously distributed, and the geographical gaps between habitats are likely a major component of the evolution of the region's biota (Amaral et al., 2018; Pie et al., 2018). Between the mountains of the southern AF, a low elevation area (< 800 m above sea level) stretches for over 300 km. This gap between mountain ranges, known as the São Paulo subtropical gap (*sensu* Amaral et al., 2018; Fig. 1) partially splits the Serra da Mantiqueira and northern portion of the Serra do Mar (hereafter Northern Mountain Block - NMB) from the Serra Geral and southern portion of the Serra do Mar (hereafter Southern Mountain Block - SMB). Climatic oscillations during the Quaternary may have

promoted connections of habitats currently isolated in these two regions, leading to multiple events of dispersal and gene flow between populations (Amaral et al., 2018). Across the gap, taxa show a spectrum of phenotypic and genetic divergence, ranging from continuous populations through allopatric species with diagnostic phenotypic differences. (Amaral et al., 2018; Amaro et al., 2012; Batalha-Filho et al., 2012; Françoso et al., 2016; Peres et al., 2015). Additionally, within each mountain block are endemic lineages that are restricted to either the NMB or SMB (Stotz et al., 1996).

The NMB and SMB are distributed over 10 degrees of latitude, with the gap between these two regions roughly positioned at the tropic of Capricorn (~23.5 degrees of latitude South). Across this gradient, there is a considerable increase in seasonality and a decrease in temperatures towards the south (Carnaval et al., 2014). The latitudinal gradient in temperature of the AF is likely affecting the elevation profile of cold-adapted species, given that populations occurring in the southern mountain block are generally more widespread to lower elevations (Amaral et al., 2018). Hence, the gap between southern AF mountain ranges divides populations occupying slightly different elevational distributions (Fig. 1) and offers an opportunity to test how mountain-specific interactions with the current- and paleo-climate shaped the genetic diversity co-distributed species.

To examine how genetic variation in birds has evolved during Quaternary climatic cycles in the AF mountains, we integrated the demographic history of co-distributed species with paleoclimatic modeling. We selected five endemic species with populations isolated by the São Paulo Subtropical Gap and distributed across the southern AF mountains. First, we modeled climatic suitability for the focal species under contemporary and paleoclimates (Last Glacial Maximum – 21,000 ya) to infer predicted changes in their elevational distributions and geographic ranges between glacial and interglacial periods. Second, using genome-wide markers for each taxon, we modeled demographic history to estimate the timing of population divergence, the degree of gene flow, and the extent of size changes over time in the NMB and SMB populations. Both data sources were used to test the hypothesis that the current configuration and historical dynamics of distinct mountain blocks (the NMB and SMB) can predict patterns of genetic diversity in elevation-limited taxa. If changes in elevational distribution of populations, linked to the climatic dynamics of a given mountain, govern genetic variation, then (1) the degree of population size change over time should be positively correlated with the change in the amount of suitable area among time periods, and (2) the populations currently occupying more broadly distributed elevational bands should accrue higher genetic diversity. In contrast, if we find that genetic diversity and changes in population sizes are not associated with the features of

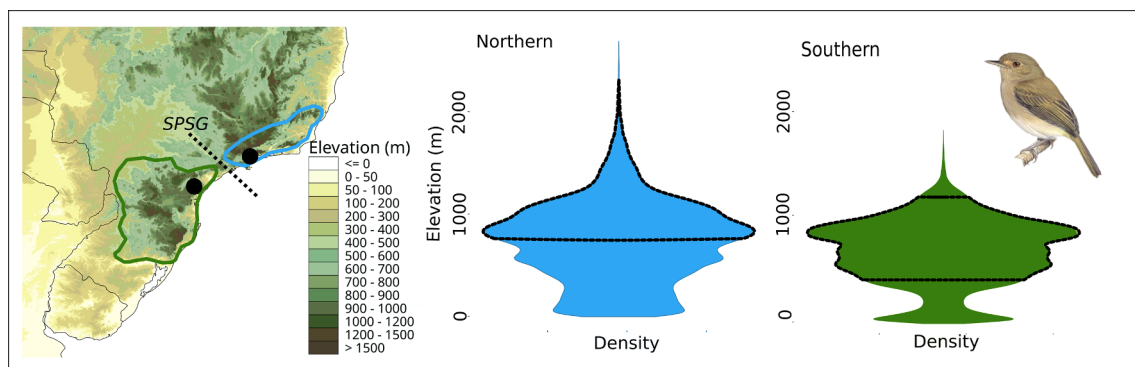


Fig. 1. Atlantic Forest mountain blocks adapted from Natural Earth's physical vectors (left panel) and symmetrical density plots representing the elevational profile of northern (NMB; center panel) and southern (SMB; right panel) mountain blocks. The dashed line on the map indicates the São Paulo subtropical gap (~23 degrees south), and black dots represent sampled localities for the molecular data. The polygons on the map represent the SMB (green) and NMB (blue) distributions. The dashed black line overlapped with the density plots represents the current elevational distribution of *Hemitriccus obsoletus* based on occurrences records and exemplifies the difference in the occupied elevations between the two mountain blocks. *Hemitriccus obsoletus* plate provided by HBW alive (<https://www.hbw.com>). (For interpretation of the references to colour in this figure legend, the reader is referred to the web version of this article.)

each mountain block, then the evolution of montane AF birds may be random with respect to changing climatic conditions. By linking demographic history to expected changes in elevational distributions over time, we demonstrate how genetic variation is associated with a complex interaction between topography and climate in a biodiversity hotspot.

2. Material and methods

2.1. Study taxa and sampling design

Here we selected five montane taxa, three of them with populations occupying the NMB and SMB (*Hemitriccus obsoletus*, *Phylloscartes difficilis*, *Castanozoster thoracicus*) and two sister species complexes structured by the mountain blocks (*Stephanoxis lalandi* and *S. loddigesii*, and *Microspingus lateralis* and *M. cabanisi*; Fig. 2). For each of the five taxon pairs, we selected five individuals from each mountain block, except *C. thoracicus*, for which we included eight individuals for the northern population, yielding a total of 53 individuals (Table S1). Samples were obtained from localities nearby the São Paulo Subtropical Gap to increase the likelihood of observing recent gene flow (Fig. 1).

2.2. Species and environmental data collection

To evaluate the extent by which climatic oscillations might have affected the geographic distribution of populations within the two

southern AF mountain ranges, we generated a set of species distribution models (SDMs) and projections to the Last Glacial Maximum (LGM). From these SDMs, we also estimated the elevational profile of populations restricted to the distinct mountain blocks. Locality records were obtained from the Global Biodiversity Information Facility (GBIF, <http://www.gbif.org>). We filtered out points outside the species known distribution or known elevational distribution. To build SDMs, we used Wallace v1.0.6 (Kass et al., 2018) in R, which allows for a straightforward implementation of several R packages and functions for estimating SDMs. To reduce sampling biases and homogenize the density of records across space we applied the spatial thinning algorithm in spThin v0.1.0.1, using a 10 km distance (Aiello-Lammens et al., 2015). We selected eight environmental variables with a spatial resolution of 2.5' retrieved from the WorldClim database (Hijmans et al., 2005). The variables are as follows: Annual Mean Temperature (Bio1), Temperature Seasonality (Bio4), Mean Temperature of Warmest Quarter (Bio10), Mean Temperature of Coldest Quarter (Bio11), Annual Precipitation (Bio12), Precipitation Seasonality (Bio15), Precipitation of Wettest Quarter (Bio16), Precipitation of Driest Quarter (Bio17). We used these eight bioclimatic variables out of the 19 that are available in the WorldClim database in order to have the same variables as the paleo-layers (i.e., HadCM3 projection).

To estimate the current and past habitat suitability, we used Maxent v3.4.1 (Phillips and Dudík, 2008). To avoid the inclusion of unoccupied suitable areas in the analyses (Peterson et al., 2011), we set a background consisting of a minimum convex polygon of the occurrence

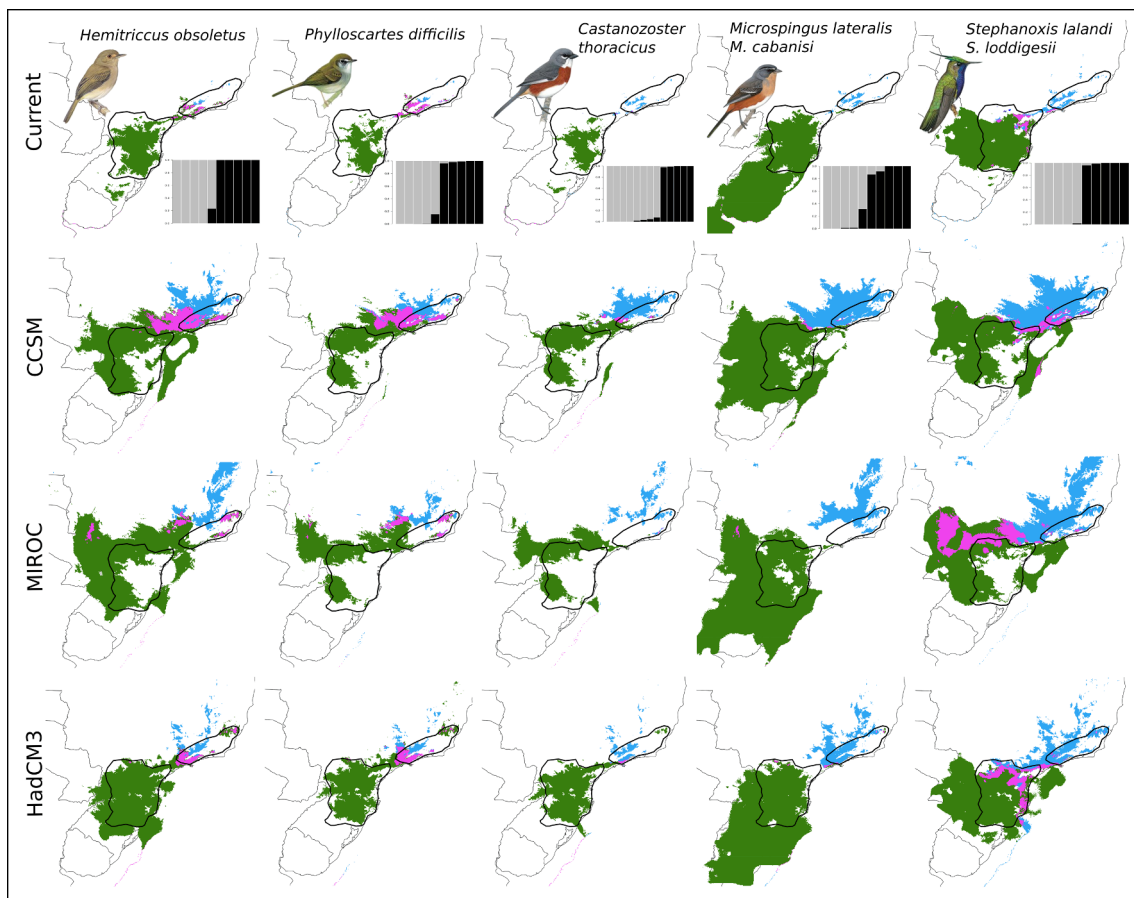


Fig. 2. Current and past (LGM) projected species distribution models and the estimated coefficient of ancestry ($K = 2$) for the five studied species. Predominantly gray bars represent individuals from the northern mountain block and predominantly black bars represent individuals from southern mountain block. Projected climatic conditions for the Last Glacial Maximum (CCSM, MIROC, and HadCM3) based on the presence-absence using the 10th percentile training presence threshold. The parameters of the best model for each population are described in Table 1. Green—southern populations; Blue—northern populations; Pink—overlap between these two SDMs. Bird plates are from HBW alive (<https://www.hbw.com>). Polygons represent the assumed geographic distribution of the northern (NMB) and southern (SMB) mountain blocks. (For interpretation of the references to colour in this figure legend, the reader is referred to the web version of this article.)

localities buffered by 0.5 degrees (~55 km). From the background area, 10,000 random points were sampled and used in the training process of the models. For populations with more than 20 occurrences, we partitioned the data into five equal portions using the random k-fold cross-validations for model training and testing (Radosavljevic and Anderson, 2014). For populations with less than 20 occurrences, we trained and tested the models using the jackknife algorithm (Shcheglovitova and Anderson, 2013).

To avoid model overfitting, while maximizing its capacity to identify suitable areas, we evaluated distinct combinations of feature classes and regularization multipliers using the R package ENMeval v0.3.0 (Muscarella et al., 2014). We explored regularization multipliers between 1 and 4 with 0.5 increments and the following feature classes: 'Linear', 'Linear + Quadratic', 'Hinge', 'Linear + Quadratic + Hinge' and 'Linear + Quadratic + Hinge + Product'. We selected the best combination of regularization multipliers and feature classes using a hierarchical combination of methods to reduce model overfitting while maximizing model accuracy (Galante et al., 2018). First, to reduce model overfitting, we assessed the value of the omission rate at the 10% omission threshold (Pearson, 2007; Radosavljevic and Anderson, 2014; Shcheglovitova and Anderson, 2013). Second, to maximize the model's discriminatory ability between true presence and the background, we filtered models by the "maximum test AUC" (area under the receiver-operating characteristic – ROC – curve; Peterson et al., 2011). Third, we used the corrected Akaike Information Criterion (AICc). Final models for each population were run with the settings identified as optimal based on the above model selection procedure using all occurrence records (without splitting the occurrences into training and testing datasets). Final models were projected to a wider geographic distribution than the initial background, between the latitude degrees –15 and –40 and longitude degrees –39 and –65.

To estimate the LGM climatic conditions, we performed a comparative approach, past projecting current niche models using three different general circulation models, the Community Climate System Model (CCSM; Collins et al., 2006), the Model of Interdisciplinary Research on Climate (MIROC; Hasumi and Emori, 2004) and the Hadley Center Climate Model (HadCM3; Singarayer and Valdes, 2010). To avoid over-extrapolation of the present and past SDM projections, we used a multivariate environmental similarity surface (MESS) analysis (Elith et al., 2010). This analysis was conducted to check whether the estimated projections contained combinations of climatic variables not represented by the training dataset. The MESS analysis indicates the locations with analogous and non-analogous habitats in relation to the training points (Elith et al., 2010; Elith and Leathwick, 2009). Only pixels with values > 0 in the MESS analysis were retained in the final projections removing any extrapolation from the models, represented by negative values. All present and past projections were converted to binary presence-absence using the 10th percentile training presence threshold for each taxon (Pearson, 2007).

To explore if populations of the same species occur at different elevations in the NMB and SMB, we estimated the current and past elevational distribution within each of these mountain ranges. Climate projections were overlaid with SRTM data, masked by the mountain blocks polygons. To evaluate if the elevational distribution changed between the LGM and the present we conducted a Kruskal-Wallis test in R, after assessing the normality of the data. Additionally, we calculated the total area in km² of the binary projection for the present and GCM projections in QGIS (QGIS Geographic Information System; Open Source Geospatial Foundation Project; <http://qgis.osgeo.org>) with the `r.report` function. Most of our environmental analyses were constrained to the distribution of the two mountain blocks of the southern AF given that 1) most of the current distribution of the five studied species is restricted to the two blocks (but see *M. cabanisi*), 2) that any oscillation in the elevation profile of the species probably occurred within these two regions, and 3) it is difficult to predict how non-occupied suitable areas (e.g. surrounding mountain ranges with similar climate but

distinct environments) were accessible for colonization over time.

We estimated the current elevational profile of the two southern AF mountain blocks by adapting the proposed mountain distributions from Natural Earth's physical vectors (version 3.0.0; available at <http://naturalearthdata.com>) to match the geographic distribution of the studied taxa. We extracted elevation data from the two mountain ranges polygons by overlaying them with high-resolution SRTM data in raster v3.0–7 (SRTM30, 30 arcsec resolution (Farr et al., 2007; Hijmans and van Etten, 2013) in R v3.5 (R Core Team, 2019).

2.3. Ultraconserved elements, bioinformatics, and genetic structure

To obtain genetic markers we performed the sequence capture of ultraconserved elements (UCEs; Faircloth et al., 2012). Genomic DNA was extracted from breast muscle using the QIAGEN DNeasy tissue and Blood kit (Valencia, CA) and quantified in Qubit 2.0 fluorometer. UCE library preparation and Illumina sequencing were outsourced to RAPiD Genomics (Gainesville, FL, USA), following the standard protocol of Faircloth et al. (2012). For four taxa, we used a probe set targeting 2312 UCEs and 97 additional probes targeting exons typically used in avian phylogenetic studies (Hackett et al., 2008; Kimball et al., 2009). For *M. lateralis*/*M. cabanisi* we used a subset of individuals from a previous study, which used a custom probe set containing 600 randomly selected UCE loci (Amaral et al., 2018). These libraries were sequenced on Illumina HiSeq 2500 (150 bp paired-end). Initial data processing and bioinformatics for SNP calling followed Thom et al. (2018): (1) read quality was evaluated in FastQC 0.11.4 (Andrews, 2014); (2) low-quality reads were excluded and sequencing adapters removed using Illuminaprocessor (Faircloth et al., 2012); (3) *de novo* assembly was performed in Trinity 2.4 (Grabherr et al., 2011); (4) contigs were matched to UCE probes, aligned with MAFFT (Katoh and Standley, 2013), and exported in fasta format with PHYLUC 1.4 (Faircloth et al., 2012). We selected the longest sequence for each locus per species to be used as a reference for the SNP calling approach. To obtain a matrix with a single SNP per locus, we aligned filtered reads with the obtained reference per species using BWA (Li and Durbin, 2009), combined all individuals per species in a single BAM file and called SNPs using the Genome Analysis Toolkit (GATK 3.6; McKenna et al., 2010), hard-masked low-quality bases (< Q30) and removed loci with read depth < 4. Finally, we randomly selected one SNP per locus, excluding sites with missing data.

To obtain full UCE sequences with phased haplotypes, we applied a custom pipeline. First, we aligned the cleaned reads of each individual with the UCE references in BWA, and used Picard (Broad Institute, Cambridge, MA; <http://broadinstitute.github.io/picard/>) to trim read ends covering regions not represented by the reference (CleanSam.jar), reassigned reads to groups (AddOrReplaceReadGroups.jar) and excluded duplicated reads (MarkDuplicates.jar). We called SNPs for each individual using UnifiedGenotyper in GATK. To output all sites, and explicitly incorporate missing data in the monomorphic sites for all loci, we applied the flag “-out_mode EMIT_ALL_SITES”. Sites with Phred quality score lower than 30 and read depth lower than four were assumed as missing data. We used the “ReadBackedPhasing” function of GATK to phase individuals vcf files, assuming a phase quality threshold of 20. Unphased variants were replaced by the IUPAC codes in the final sequence alignments. The final vcf files were converted to fasta format with bcftools (Li, 2011) and aligned with MAFFT (Katoh and Standley, 2013). Individuals with more than 50% missing data for a given locus were removed with Alignment_Refiner_v2.py (Portik et al., 2016), and missing data in the UCE's flanking regions were removed with trimAL (Capella-Gutierrez et al., 2009). Given that the conserved core of UCE loci has been shown to be under selection (Katzman et al., 2007), and that our demographic simulations assume neutral evolving markers, we removed the UCE probe sequences from the alignments. Despite the linkage among the conserved core and the flanking regions, we believe that excluding the core might help ameliorate the effect of possible selection.

We tested the best-fit number of ancestral populations (K) for each species complex and clustered individuals to populations in sNMF using the matrix with a single SNP per locus (Frichot et al., 2014). sNMF uses a sparse non-negative matrix factorization approach to compute least-square estimates of ancestry coefficients. We tested for the presence of one or two ancestral populations performing 100 replicates for each value of K with three distinct alpha regularization parameters, 1, 10 and 100.

2.4. Modeling demographic history

To test the demographic histories of the five focal species, we implemented a machine learning algorithm for model selection and demographic parameter estimation. We used the R package PipeMaster (Gehara et al., 2017), which uses the msABC coalescent-simulator (Hudson, 2002; Pavlidis et al., 2010) to simulate genetic data and estimate summary statistics under specific demographic scenarios. Here the phased UCE alignments were used as observed data. We simulated data under nine alternative models that describe a large suite of demographic histories and patterns of connectivity among populations restricted to the SMB and NMB (Fig. 3). For each simulation, model parameters were randomly sampled from uniform distributions. We specified broad priors for current and ancestral effective population sizes (min: 10,000, max: 2,000,000 individuals), divergence time (min:

5000, max: 1,000,000 years) and migration (min: 0.5, max: 4.0 migrants per generation; $4Nm$) that reflect uncertainty in population histories for birds during the Pleistocene. Priors for parameters associated to the time of population size change in models M4, M5 M6, M7, M8, M9 (min: 5000, max: 15,000), as well as the time of migration between populations in models M3, M5, M7, M8, M9 (min: 4000, max: 400,000), were based on the climatic variations during the last interglacial/glacial periods.

We conducted 50,000 simulations per model and calculated the following summary statistics for each species: number of segregating sites (S), nucleotide diversity (π), Watterson's theta (θ ; Watterson, 1975), Tajima's D (Tajima, 1989), pairwise F_{ST} (Wright, 1950), Fay and Wu's H (Fay and Wu, 2000), the proportion of shared alleles between populations, the proportion of private alleles in each population, and the proportion of fixed alleles in each population. To check how simulated data fit the observed data, we conducted a Principal Component Analysis (PCA) per species in R. To evaluate the accuracy of model selection we implemented a supervised machine learning approach using the nonlinear neural network algorithm on the R package caret v6.0-84 (Kuhn et al., 2017). We used the nnet algorithm, performing 20 bootstraps to estimate which combination of the number of nodes and decay value for the weights improved the accuracy of our approach. To calculate the posterior distributions of the parameters for the best models we used the neuralnet algorithm from the functions abc of the ABC v2.1 package (Csilléry et al., 2012) in R. To assess the accuracy of parameter estimation, we performed 100 cross-validations with the function cv4abc from ABC in R, and estimated Pearson's correlation index between simulated and pseudo-observed data sets. We conducted parameter estimation and cross-validations with a tolerance level of 10% of the closest simulations to the observed and pseudo-observed data.

3. Results

3.1. Species elevational distribution and SDMs

The two southern AF mountain blocks (NMB and SMB) have the highest surface density occurring at elevations between 500 and 1000 masl, with an abrupt reduction in surface area from 1000 m towards higher elevations (Fig. 1). After filtering, there were 14 (*P. difficilis*—SMB) to 158 (*M. cabanisi*—SMB) occurrence records per population with a mean number of records of 24.0 (SD = 9.97) and 74.6 (SD = 75.98) for the NMB and SMB, respectively (see supplementary material). All models had AUC for test points > 0.87 and omission rates (OR10) ranging from 0.108 to 0.222 (Table 1). The best models for each taxon supported a wider current distribution and lower mean elevational distribution for southern populations (mean elevation = 856 masl, SD = 369.58) than for northern populations (mean elevation = 1285 masl, SD = 534.12), suggesting smaller and more fragmented distributions in the NMB (Figs. 2, 4, S1; Tables S2–S3). The elevational profile estimated for each species suggests variation between species within each mountain block (Fig. 4; Table S3). The species with the most distinct elevational differences between mountain blocks was *C. thoracicus* (mean elevation at NMB = 1481 masl; mean elevation at SMB = 1044 masl), occurring on average ~ 200 m higher than the remaining species (Fig. 4; Table S3).

Past projections supported wider environmental suitability and a significant elevational change (Kruskal Wallis test P-value < 0.05; Table S3) for all populations except for *M. cabanisi*, with more substantial changes in elevation for the northern (mean = 307.8 m, SD = 160.30) than southern populations (mean = 212.33 m, SD = 152.14; Table S3; Fig. 4). The most pronounced shift in elevation was detected in *C. thoracicus*, with a mean change of 448.63 and 470.6 m for the NMB and SMB, respectively (Table S3). Except for *M. cabanisi*, all southern taxa show a drastic change in the distribution of suitable habitats in the LGM for the CCSM and MIROC projections,

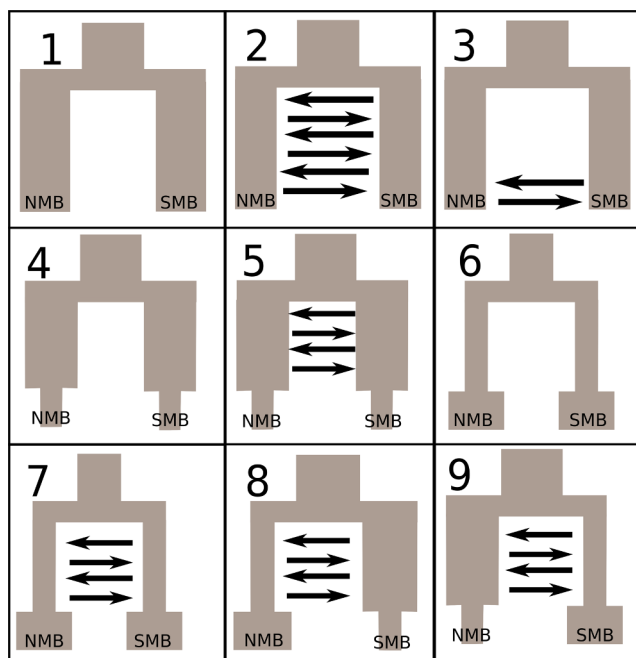


Fig. 3. Schematic of the alternative demographic models tested for each of the five studied species. Models varied the presence and timing of gene flow as well as population size changes after divergence. (1) Pure isolation— isolation between populations without subsequent secondary contact and stable population sizes after divergence; (2) Isolation migration— isolation between populations then constant gene flow between populations with population size remaining constant; (3) Isolation with secondary contact— initial isolation between populations then after a period of time gene flow occurs between populations with population size remaining constant; (4) Pure isolation and recent bottleneck in both populations— same as model 1 except that both daughter populations undergo bottlenecks; (5) Isolation with ancient migration followed by a bottleneck in both populations; (6) Pure isolation and recent demographic expansions in both populations; (7) Isolation with ancient migration followed by demographic expansions in both populations; (8) Isolation with ancient migration followed by a bottleneck in the SMB population and demographic expansion in the NMB population; (9) Isolation with ancient migration followed by a bottleneck in the NMB population and demographic expansion in the SMB population. NMB—Northern mountain block; SMB—Southern mountain block.

Table 1
Parameters of the best species distribution model for both populations in each complex.

Taxon	Population	Feature classes	RM	AUC	OR10%	AICc	N param
<i>H. obsoletus</i>	NMB	LQ	2.5	0.95	0.118	243.79	3
<i>H. obsoletus</i>	SMB	LQH	3	0.95	0.119	805.55	6
<i>P. difficilis</i>	SMB	LQ	1.5	0.95	0.222	166.23	3
<i>P. difficilis</i>	NMB	LQP	1	0.99	0.125	360.53	4
<i>M. lateralis</i>	NMB	LQ	2	0.99	0.161	462.51	3
<i>M. cabanisi</i>	SMB	LQH	1.5	0.87	0.108	3455.30	21
<i>C. thoracicus</i>	SMB	LQPH	4	0.96	0.125	149.83	2
<i>C. thoracicus</i>	NMB	LQ	2.5	0.99	0.200	133.69	1
<i>S. lalandi</i>	NMB	LQPH	4	0.99	0.114	560.57	5
<i>S. loddigesii</i>	SMB	LQP	2	0.99	0.143	568.98	4

NMB—northern mountain block; SMB—southern mountain block. LQ—Linear + Quadratic, LQH—Linear + Quadratic + Hinge, LQP—Linear + Quadratic + Product, LQPH—Linear + Quadratic + Hinge + Product; RM—regularization multipliers; AUC—area under the receiver-operating characteristic curve; OR10%—omission rate at the 10% omission threshold; AICc – corrected Akaike Information Criterion; N param—number of model parameters.

when compared to the current projected SDMs (Fig. 2). Our results support a considerably larger suitable area in the LGM than in the present for the northern populations (~8X larger) but not for the southern populations (~1.5X larger) when considering the total extension of the projected model (not clipping by the mountain area; Table S2, Figs. 2, S1). When clipping the SDMs by mountain block the difference in surface area between the LGM and the present was reduced in the NMB (~3X larger) populations and remained similar for the SMB (~1.2X larger) populations (Table S2, Figs. 2, S1). For the SMB, despite an apparent stable suitable area between projected SDMs, our data support a major habitat displacement from the currently occupied highlands towards the lowlands and the interior of the continent for the CCSM and MIROC projections (but see HadCM3 results; Fig. 2).

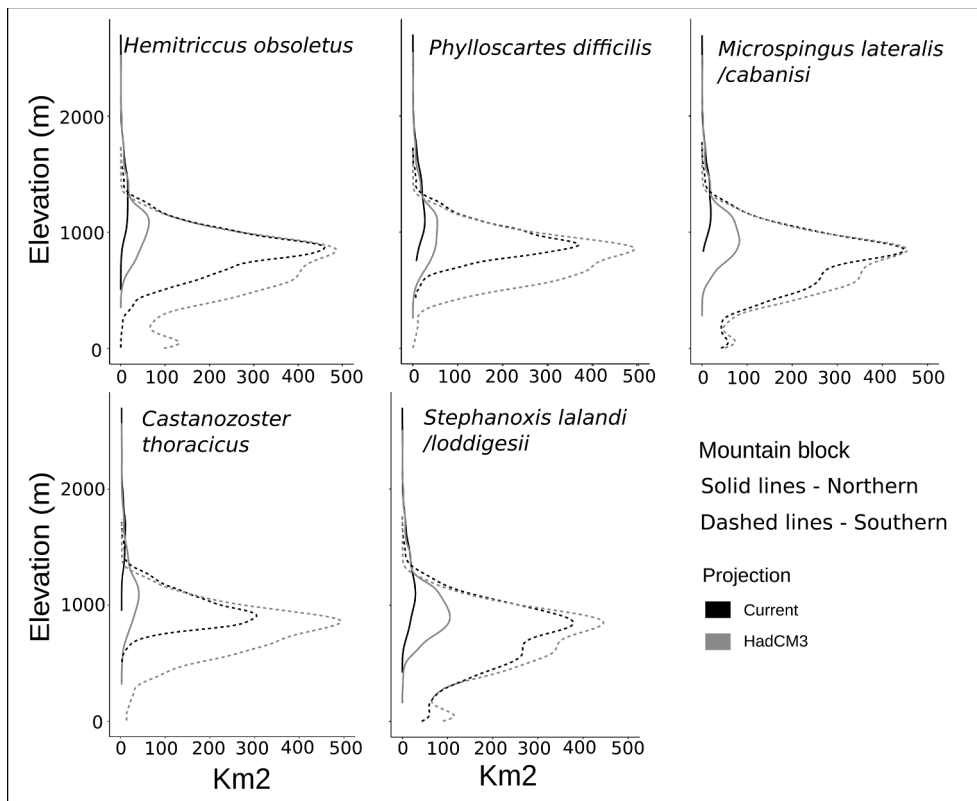


Fig. 4. Elevational profile of current and past projected (MIROC - LGM) species distributional models for the five species studied within the northern (NMB) and southern (SMB) mountain blocks of the southern Atlantic Forest. Elevational profiles for other general circulation models (CCSM and HadCM3) are available in the supplementary material (Figs. S7 and S8).

The most drastic change in the suitable area between the LGM and present projections, considering the total projected area (not clipping by the mountain area) was detected for the NMB population of *C. thoracicus* (CCSM ~18X larger in the LGM, Table S2). Connectivity between northern and southern populations, measured as the geographic overlap of the projected SDMs, varied considerably but was relatively consistent between past and present projected SDMs (Fig. 2). For example, *C. thoracicus* and *M. cabanisi*/*M. lateralis* had the smallest geographic overlap in both time periods and all three past projections (Fig. 2).

3.2. Genetic variation and population structure

Our SNP calling approach yielded an average of 5917 SNPs per species with a mean read depth of 26.8 (Table S4). When selecting a single SNP per locus without missing data, we obtained matrices with an average of 1104 SNPs per species (Table S4). The data processing to obtain phased UCE sequences without the conserved probes within alignments yielded on average 1975 loci per species with a mean size of 373 bp, containing 2.6 SNPs per loci on average (Table S4).

The sNMF analyses supported $K = 2$ as the best clustering scheme for all five taxa with $\alpha = 10$ producing the lowest cross-validation values, clustering the northern and southern individuals in distinct populations (Fig. 2). Summary statistics indicated that genetic diversity was higher in the southern populations (Table 2). The average number of segregating sites per locus varied from 0.743 in *H. o. obsoletus* (northern population) to 2.636 in *M. cabanisi* (southern population; Table 2). Average F_{ST} ranged from 0.057 between *P. difficilis* populations to 0.199 between *C. thoracicus* populations (Table 2).

3.3. Historical demography

The best-fit demographic model varied among species, especially regarding the presence of gene flow and population size changes (Table 3). For *H. obsoletus*, the model with the highest probability

Table 2

Average summary statistics of UCEs for the populations in the northern mountain block (NMB) and southern mountain block (SMB).

Taxon	# segregating sites	Pi	Watterson's theta	Tajima's D	Fst	Private alleles	Fixed alleles
<i>H. obsoletus</i> NMB	0.743	0.258	0.263	-0.086	0.094	0.855	0.0075
<i>H. obsoletus</i> SMB	0.924	0.319	0.327	-0.125			
<i>P. difficilis</i> NMB	0.956	0.322	0.338	-0.187	0.057	0.836	0.0001
<i>P. difficilis</i> SMB	1.300	0.433	0.460	-0.235			
<i>M. lateralis</i> NMB	2.329	0.815	0.823	-0.105	0.060	0.819	0.0002
<i>M. cabanisi</i> SMB	2.636	0.892	0.932	-0.209			
<i>C. thoracicus</i> NMB	1.397	0.371	0.421	-0.354	0.199	0.874	0.0385
<i>C. thoracicus</i> SMB	1.664	0.586	0.588	-0.041			
<i>S. lalandi</i> NMB	1.554	0.518	0.549	-0.223	0.148	0.885	0.0228
<i>S. loddigesii</i> SMB	1.600	0.540	0.565	-0.200			

Table 3

Model classification probability obtained with a supervised machine learning approach using a neural network algorithm. Models are described in Fig. 2.

Taxon	m1	m4	m5	m6	m7	m8	m9	m2	m3	Overall Accuracy	Kappa	Best model accuracy
<i>H. obsoletus</i>	0.00	0.00	0.00	0.13	0.18	0.07	0.61	0.00	0.00	0.62	0.58	0.79
<i>P. difficilis</i>	0.00	0.00	0.00	0.11	0.24	0.07	0.03	0.50	0.04	0.62	0.57	0.87
<i>M. lateralis/M. cabanisi</i>	0.00	0.00	0.00	0.25	0.52	0.13	0.10	0.00	0.00	0.59	0.53	0.78
<i>C. thoracicus</i>	0.25	0.00	0.00	0.54	0.15	0.00	0.06	0.00	0.00	0.60	0.55	0.76
<i>S. lalandi/S. loddigesii</i>	0.00	0.00	0.00	0.67	0.24	0.09	0.00	0.00	0.00	0.61	0.57	0.80

(model 9—probability (P) = 0.61) supported the presence of ancient gene flow followed by an expansion in the southern population and a contraction in the northern population. For *P. difficilis* the best model (Model 2—P = 0.5), supported an isolation-migration model, without population size changes. For *M. cabanisi/M. lateralis*, the model with the highest probability (model 7—P = 0.52) included the presence of ancient gene flow and population expansion for both populations. For *C. thoracicus* and *S. lalandi/S. loddigesii* the best model (model 6—P = 0.54 and 0.67 for *C. thoracicus* and *S. lalandi/S. loddigesii*, respectively) supported the absence of gene flow since divergence and recent population expansions in both populations (Table 3).

Parameter estimation for the best models supported a relatively high variation among species for divergence times and gene flow. Divergence between populations occurred in the Mid and Late Pleistocene and varied between species. The most recent divergence events were estimated for *M. lateralis/M. cabanisi* (median = 43,879 ya, 95% CI = 2250–84,861 ya) and *S. lalandi/S. loddigesii* (median = 81,696 ya, 95% CI = 57,583–208,664 ya), followed by *C. thoracicus* (median = 251,650 ya, 95% CI = 394,448–443,960 ya), *P. difficilis* (median = 303,171 ya, 95% CI = 175,326–438,420 ya) and *H. obsoletus* (median = 482,492 ya, 95% CI = 157,692–842,101 ya; Table S5; Fig. 5). The presence of gene flow was observed in three species, *H. obsoletus*, *P. difficilis* and *M. lateralis/M. cabanisi* (Table S5).

We detected more variation in historical demography between populations of the same species occurring in distinct mountain blocks than between populations of different species within the same mountain blocks. For most of the NMB populations, the best model included demographic expansions, but the 95% credibility interval for current and ancestral population sizes largely overlapped, suggesting mild oscillations (range for population size variation between current and ancestral population = 1.1X to 2.35X; Table S5; Fig. 5) or even stable populations in the NMB. On the contrary, population expansions in the SMB were considerably more pronounced, with current populations being on average 6.78X (range from 3.22X to 10.64X) larger than ancestral populations (except for *P. difficilis*; Table S5; Fig. 5). The estimated time for population size changes in SMB populations varied from ~42,000 ya (median, 95% CI = 7194–80,567 ya) in *M. cabanisi* to ~111,000 ya (median, 95% CI = 71,617–148,195 ya) in *S. loddigesii* (Table S5).

The PCAs showed that simulated summary statistics fit the data well, with the observed data clustering together with the simulations in the first four PCs for all species (Figs. S2–S6). Our neural network approach for model selection showed that the nine models were correctly classified with a 60% accuracy for all five species (Table 3). The confusion matrices indicated that the decrease in accuracy was caused by misclassification among similar models (Fig. S7). For example, models 4 and 5, which both included recent bottlenecks in both populations,

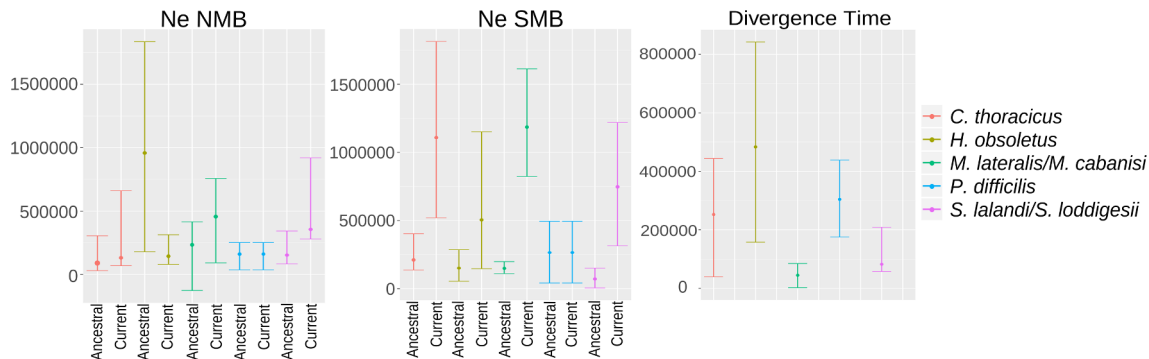


Fig. 5. Mean and 95% credibility interval of the posterior distribution for estimated effective population sizes for the northern (NMB) and southern (SMB) mountain blocks populations, including ancestral (before population size change to occur forward in time) and current populations, and divergence times between SMB and NMB. The absolute numbers for each parameter are available in Table S5.

were largely confounded (Fig. S7). Similarly, models 6 and 7, which included recent expansions for both populations were often misclassified (Fig. S7). Correlations between pseudo-observed and simulated data obtained through the 100 cross-validations for parameter estimations suggested that most of the parameters for divergence time and effective population size were correctly estimated (Table S6, Pearson's correlation coefficient > 0.7). However, parameters associated with gene flow, including the amount and timing for gene flow to cease towards the present, had relatively low Pearson's correlation coefficient (< 0.7) among pseudo-observed and simulated data sets. The relatively low correlation coefficient suggested that despite the good accuracy of our approach for identifying models with gene flow, the absolute estimation of these parameters was limited (Table S6).

4. Discussion

Our findings showed that historical population size changes in montane AF birds are attributable to the amount of suitable area among time periods and the current elevational distribution of each population. In the contemporary configuration of the southern AF montane habitats, populations in the SMB have more widespread elevational distributions, occur at lower elevations, and consequently harbor higher levels of genetic diversity than NMB populations. The more intense demographic fluctuations inferred for the SMB populations was consistent with our paleoclimatic modeling, which indicated that habitats were more dynamic in the south. Despite the apparent coupling of demographic and climatic oscillations, our data also suggest that the species had various modes of differentiation among mountain blocks, a pattern inconsistent with a simultaneous evolutionary response to glacial cycles. All five focal species in this study showed genetic structuring across the São Paulo subtropical gap but varied in the timing of divergence and the degree of gene flow across the barrier. Collectively, our results show how landscape history can enact as an evolutionary control on genetic variation in the face of idiosyncratic responses to dynamic environments.

4.1. Conflicting relationship with climate dynamics

We found conflicting evidence for the influence of climatic cycles on the population history of AF montane birds. Under a simplistic scenario, sky island communities are predicted to be synchronously isolated during glacial cycles by habitat fragmentation (Hewitt, 2004). Our demographic models and parameter estimates do not support these predictions but instead, favor alternative explanations for the drivers of population structuring among mountain blocks. Disparity in divergence times and gene flow regimes among these co-distributed species may be attributable to differences in life-history traits associated with propensity to move across the landscape (Burney and Brumfield, 2009; Paz et al., 2019), differences in the length of time each lineage has been in the southern AF, and/or an interaction between species ecology and history (Smith et al., 2014). The factors responsible for the variation in the mode of differentiation do not appear to be operating at a shallower evolutionary time frame. We found strong congruence in demographic changes in each mountain block that were consistent with the availability of habitat across time periods. At this scale, all species have a comparable history in landscape and the influence of dispersal ability on genetic diversity may be minimized by the impacts of widespread displacement caused by climatic cycles. For example, based on divergence times, all five species were present in each mountain block since at least the Late Pleistocene. By modeling the demographic history of each species a more nuanced pattern was uncovered that further clarifies how distinct factors shape different axes of population history.

4.2. Genetic diversity is associated with distinct mountain blocks

Our data show that species have different demographic patterns in

each of the mountain blocks (except for *P. difficilis*; Table S5). This pattern is explainable by the contemporary elevational distribution of populations in SMB and NMB, and how these elevational distributions were inferred to be impacted by climatic oscillations (Figs. 2, 4; Janzen, 1967; Polato et al., 2018). In the SMB, populations are more widespread and occur at lower elevations, and are presumably more connected than those occurring in the NMB. The parameter estimates from our demographic models corroborate this prediction, with the SMB harboring populations with larger effective population sizes than the NMB. Our models indicate that in the SMB, there was a major change in the geographic location of suitable areas, during the LGM (except for HadCM3; Fig. 2), with the exclusion of adequate habitats from currently occupied areas. This matches our best demographic models that supported more pronounced demographic expansions for most of the SMB populations (Table 3). For the populations occurring in the NMB (Fig. 2), demographic parameters supported more stable population sizes over time when compared with SMB populations (Table S5; Fig. 5). These results suggest that populations occupying the colder and more seasonal SMB might be more susceptible to colder historical climatic conditions than populations occurring in the NMB (Fig. S1). According to our projected SDMs, the LGM conditions removed suitable habitats from the southernmost portions of the species distribution as well as from the higher elevations of the Serra Geral. Our findings are contrary to the expectations for a sky-island system during Quaternary climate change, which predicts the expansion of montane habitats during colder conditions (Hewitt, 2004) (Fig. S1).

The classical expectation for patterns of genetic variation in sky-island systems predicts a loss of diversity since the Last Glacial Maximum, irrespective of the elevational band occupied (Hewitt, 2004). This latter prediction assumes a pyramidal shape of the mountain range and states that the current interglacial conditions have forced cold-adapted species towards higher elevations (Şekercioğlu et al., 2012). However, the elevational profiles in the AF mountains do not follow a linear reduction in the surface area up mountains (Fig. 1), with the highest surface area density at mid-high elevations, due to the presence of plateaus (~500–1000 m; Fig. 1; Elsen and Tingley, 2015). The large surface area at mid-high elevations may help ameliorate the impacts of climatic cycles by maintaining microhabitats that function as a buffer for organisms to track optimal thermic zones (Elsen and Tingley, 2015; Wiens et al., 2007). This buffering mechanism might be more effective in the lower latitudes of the NMB, where seasonality is less pronounced (Janzen, 1967; Polato et al., 2018; Roy et al., 1997). Our results agree with this scenario, with NMB populations having relatively more stable sizes or contractions (based on parameter estimations) than SMB populations, the latter of which increased approximately 6X since the LGM (except for *P. difficilis*; Table S5; Fig. 5).

4.3. Sampling considerations

Despite a large number of loci and the identifiability of the tested models, our sampling scheme has limitations worth acknowledging. We focused our sampling efforts near the São Paulo Subtropical Gap to increase the likelihood of capturing gene flow among mountain blocks. However, limiting the geographic area of sampling could have produced biased estimates that do not represent the demography of the entire population. For instance, populations facing geographic expansions associated with the glacial-interglacial dynamics could be subjected to successive founder events leaving distinct demographic signatures across their distributions (Excoffier et al., 2009). Similarly, subpopulations isolated in distinct mountain regions could be differently impacted by genetic drift, depending on the available area in the mountain. Our climatic reconstructions suggested that the SMB sampled locality is in a region with an unsuitable climate during the LGM for four of the five species (but see HadCM3 projections; Fig. 2), implying recent colonization that could explain the more pronounced demographic expansions in the area (Excoffier et al., 2009). On the

contrary, our projections for four of the five species indicated that the NMB sampled locality was climatically more stable, which is consistent with our demographic modeling that did not find evidence of strong population expansions in the region. Additional sampling, along with spatially-explicit methods, could further elucidate the spatial distribution of genetic variation in the AF and clarify how past climatic oscillations drive contrasting local dynamics.

Despite the potential limitations of our sampling scheme, we found an uncommon pattern with distinct population dynamics associated with different mountain blocks with characteristic climatic regimes (Fig. S1). Previous studies on AF montane organisms in general reported stable climatic conditions in the southern AF since the Last Interglacial Maximum or habitat expansion during the LGM (Amaro et al., 2012; Batalha-Filho et al., 2012; Carnaval et al., 2009; Leite et al., 2016; Paz et al., 2019). Similarly, a recent study using the same molecular markers but with a denser geographic sampling of *M. lateralis*/*M. cabanisi* recovered similar gene flow levels between species, divergence times, and population sizes to the ones reported here, but rejected models with population size changes (Amaral et al., 2018). However, in accordance with our results, a study on AF montane bumblebees of the genus *Bombus* supported an asynchrony in habitat size changes between the SMB and NMB (Françoso et al., 2016). While the southern population expanded its distribution during the warmer conditions of the Last Interglacial Maximum, the northern population expanded its distribution during the LGM (Françoso et al., 2016). The heterogeneity of patterns reported here coupled with previous studies supports that the southern AF biota is a product of multiple histories, likely not exclusively linked to the landscape evolution.

4.4. Regionalization of AF montane environments

Our data support that recently evolved lineages share similar patterns of distribution, adding a new layer to the AF biogeographic regions (Carnaval et al., 2014). The AF is characterized by the presence of two bioclimatic domains with distinct fauna and flora (Carnaval et al., 2014). The portion of the biome northern from the Rio Doce region is warmer and has widespread lowlands that share biotic components with eastern Amazonia (Batalha-Filho et al., 2013). In contrast, the southern portion has a more seasonal climate and the prevalence of montane and sub-tropical species related to Andean lineages (Batalha-Filho et al., 2013; Carnaval et al., 2014). In addition to this major biogeographic division of the AF, our data supported further sub-structure within the South, with contrasting climatic variation between NMB and SMB (Fig. S1). Phylogenetic and phylogeographic studies have recovered multiple lineages exclusive to the SMB or NMB, suggesting that the biota of these two mountain blocks are evolving independently (Amaral et al., 2018; Amaro et al., 2012; Cavazere et al., 2014; Françoso et al., 2016; Paz et al., 2019; Pie et al., 2018). The contrasting climate among northern and southern mountain blocks could also affect patterns of local adaptation, promoting faster differentiation among populations (Nosil, 2012). Studies testing niche evolution could provide the means to understand if the distinct elevational distribution among populations is a compensation associated with the latitudinal gradient of the AF, or if lineages are diverging in ecological traits. Future work focusing on geographic variation of adaptive traits in each climatic regime may clarify the observed variation in historical demography and gene flow regimes among populations in each mountain block (Nosil, 2012; Strangas et al., 2019; Tieleman et al., 2003).

Declaration of Competing Interest

The authors declare that they have no known competing financial interests or personal relationships that could have appeared to influence the work reported in this paper.

Acknowledgements

We thank the curator and curatorial assistants of the Laboratório de Genética e Evolução Molecular de Aves (LGEMA) and Museu de Zoologia da Universidade de São Paulo (MZUSP) for allowing us to borrow tissue samples and study specimens under their care. We thank members of the Smith lab and Carnaval lab, Kaiya L. Provost, Lucas R. Moreira, Vivien Chua, and Jon Merwin, Ana C. Carnaval, Connor French, Andrea Paz, Kathryn Mercier, Rilquer Mascarenhas, and Lidia Martins. This work was partially developed in the Research Center on Biodiversity and Computing (BioComp) of the Universidade de São Paulo (USP), supported by the USP Provost's Office for Research. Specimens were collected under the ICMBio/SISBIO permanent collecting permits 30835-3 and 47205-1 and approved by the Animal Ethics Committee of the University of São Paulo, protocol #188/2013, as well as the Animal Ethics Committee of the Federal University of São Paulo (CEP 0069/12 and CEUA 6433170817).

Funding

This study was co-funded by FAPESP and the BIOTA program (2011/50143-7, 2011/23155-4, 2013/50297-0, 2018/03428-5), CNPq/MCTIC research productivity fellowship (312697/2018-0; 303713/2015-1), Coordenação de Aperfeiçoamento de Pessoal de Nível Superior - Brasil (CAPES) - Finance Code 001, NASA through the Dimensions of Biodiversity Program of the National Science Foundation (DOB 1343578, DOB 1831560). GT was granted by FAPESP scholarships (2018/17869-3, 2017/25720-7) and Frank M. Chapman memorial fund of the American Museum of Natural History. MSL-R research has been funded by CNPq (proc. 426785/2018-5) and the National Institutes for Science and Technology (INCT) in Ecology, Evolution and Biodiversity Conservation, supported by MCTIC/CNPq (465610/2014-5) and FAPEG (201810267000023).

Data and materials availability

All data needed to evaluate the conclusions of this study are present in the manuscript and/or the [Supplementary Materials](#). Additional data related to this paper will be available at <https://github.com/GregoryThom/> or may be requested from the authors. All genetic data is available in the Short Read Archive (SRA, Submission #SUB6731963, BioProject #PRJNA597755).

Appendix A. Supplementary material

Supplementary data to this article can be found online at <https://doi.org/10.1016/j.ympcv.2020.106812>.

References

- Aiello-Lammens, M.E., Boria, R.A., Radosavljevic, A., Vilela, B., Anderson, R.P., 2015. spThin: an R package for spatial thinning of species occurrence records for use in ecological niche models. *Ecography* 38, 541–545. <https://doi.org/10.1111/ecog.01132>.
- Alves, L.F., Vieira, S.A., Scaranello, M.A., Camargo, P.B., Santos, F.A.M., Joly, C.A., Martinelli, L.A., 2010. Forest structure and live aboveground biomass variation along an elevational gradient of tropical Atlantic moist forest (Brazil). *For. Ecol. Manage.* 260, 679–691. <https://doi.org/10.1016/j.foreco.2010.05.023>.
- Amaral, F.R., Alvarado-Serrano, D.F., Maldonado-Coelho, M., Pellegrino, K.C.M., Miyaki, C.Y., Montesanti, J.A.C., Lima-Ribeiro, M.S., Hickerson, M.J., Thom, G., 2018. Climate explains recent population divergence, introgression and persistence in tropical mountains: phylogenomic evidence from Atlantic Forest warbling finches. *bioRxiv*. <https://doi.org/10.1101/439265>.
- Amaro, R.C., Rodrigues, M.T., Yonenaga-Yassuda, Y., Carnaval, A.C., 2012. Demographic processes in the montane Atlantic rainforest: molecular and cytogenetic evidence from the endemic frog *Proceratophrys boiei*. *Mol. Phylogenet. Evol.* 62, 880–888. <https://doi.org/10.1016/j.ympcv.2011.11.004>.
- Andrews, S., 2014. FastQC: a quality control tool for high throughput sequence data. Version 0.11. 2. Babraham Institute, Cambridge, UK <http://www.bioinformatics.babraham.ac.uk/projects/fastqc>.

- Badgley, C., Smiley, T.M., Terry, R., Davis, E.B., DeSantis, L.R.G., Fox, D.L., Hopkins, S.S.B., Jezkova, T., Matocq, M.D., Matzke, N., McGuire, J.L., Mulch, A., Riddle, B.R., Roth, V.L., Samuels, J.X., Strömberg, C.A.E., Yanites, B.J., 2017. Biodiversity and Topographic Complexity: Modern and Geohistorical Perspectives. *Trends Ecol. Evol.* 32, 211–226. <https://doi.org/10.1016/j.tree.2016.12.010>.
- Batalha-Filho, H., Cabanne, G.S., Miyaki, C.Y., 2012. Phylogeography of an Atlantic forest passerine reveals demographic stability through the last glacial maximum. *Mol. Phylogenet. Evol.* 65, 892–902. <https://doi.org/10.1016/j.ympev.2012.08.010>.
- Batalha-Filho, H., Fjeldså, J., Fabre, P.-H., Miyaki, C.Y., 2013. Connections between the Atlantic and the Amazonian forest afaunans represent distinct historical events. *J. Ornithol.* <https://doi.org/10.1007/s10336-012-0866-7>.
- Behling, H., Dupont, L., Safford, H.D., Wefer, G., 2007. Late Quaternary vegetation and climate dynamics in the Serra da Bocaina, southeastern Brazil. *Quat. Int.* <https://doi.org/10.1016/j.quaint.2006.10.021>.
- Behling, H., Pillar, V.D., 2007. Late Quaternary vegetation, biodiversity and fire dynamics on the southern Brazilian highland and their implication for conservation and management of modern Araucaria forest and grassland ecosystems. *Philosophical Trans. Royal Soc. B: Biol. Sci.* <https://doi.org/10.1098/rstb.2006.1984>.
- Behling, H., Safford, H.D., 2010. Late-glacial and Holocene vegetation, climate and fire dynamics in the Serra dos Órgãos, Rio de Janeiro State, southeastern Brazil. *Glob. Chang. Biol.* 16, 1661–1671.
- Burney, C., Brumfield, R., 2009. Ecology predicts levels of genetic differentiation in Neotropical birds. *Am. Natural.* 174 (3), 358–368. <https://doi.org/10.1086/603613>.
- Cadena, C.D., Kozak, K.H., Gómez, J.P., Parra, J.L., McCain, C.M., Bowie, R.C.K., Carnaval, A.C., Moritz, C., Rahbek, C., Roberts, T.E., Sanders, N.J., Schneider, C.J., VanDerWal, J., Zamudio, K.R., Graham, C.H., 2012. Latitude, elevational climatic zonation and speciation in New World vertebrates. *Proc. Royal Soc. B: Biol. Sci.* <https://doi.org/10.1098/rspb.2011.0720>.
- Capella-Gutiérrez, S., Silla-Martínez, J.M., Gabaldón, T., 2009. trimAl: a tool for automated alignment trimming in large-scale phylogenetic analyses. *Bioinformatics.* <https://doi.org/10.1093/bioinformatics/btp348>.
- Carnaval, A.C., Hickerson, M.J., Haddad, C.F.B., Rodrigues, M.T., Moritz, C., 2009. Stability predicts genetic diversity in the Brazilian Atlantic forest hotspot. *Science* 323, 785–789. <https://doi.org/10.1126/science.1166955>.
- Carnaval, A.C., Waltari, E., Rodrigues, M.T., Rosauer, D., VanDerWal, J., Damasceno, R., Prates, I., Strangas, M., Spanos, Z., Rivera, D., et al., 2014. Prediction of phylogeographic endemism in an environmentally complex biome. *Proc. Royal Soc. B: Biol. Sci.* 281, 20141461.
- Cavazzere, V., Silveira, L.F., de Vasconcelos, M.F., Grantsau, R., Straube, F.C., 2014. Taxonomy and biogeography of *Stephanoxis* Simon, 1897 (Aves: Trochilidae). *Pap. Avulsos Zool.* 54.
- Cheng, H., Sinha, A., Cruz, F.W., Wang, X., Edwards, R.L., d'Horta, F.M., Ribas, C.C., Vuille, M., Stott, L.D., Auler, A.S., 2013. Climate change patterns in Amazonia and biodiversity. *Nat. Commun.* 4, 1411. <https://doi.org/10.1038/ncomms2415>.
- Chen, I.-C., Chen, I.-J., Shiu, H., Benedick, S., Holloway, J.D., Chey, V.K., Barlow, H.S., Hill, J.K., Thomas, C.D., 2009. Elevation increases in moth assemblages over 42 years on a tropical mountain. *Proc. National Acad. Sci.* <https://doi.org/10.1073/pnas.0809320106>.
- Colinvaux, P.A., Bush, M.B., Steinitz-Kannan, M., Miller, M.C., 1997. Glacial and Postglacial Pollen Records from the Ecuadorian Andes and Amazon. *Quat. Res.* 48, 69–78. <https://doi.org/10.1006/qres.1997.1908>.
- Collins, W.D., Bitz, C.M., Blackmon, M.L., Bonan, G.B., Bretherton, C.S., Carton, J.A., Chang, P., Doney, S.C., Hack, J.J., Henderson, T.B., Kiehl, J.T., Large, W.G., McKenna, D.S., Santer, B.D., Smith, R.D., 2006. The Community Climate System Model Version 3 (CCSM3). *J. Clim.* 19, 2122–2143. <https://doi.org/10.1175/JCLI3761.1>.
- Csilléry, K., François, O., Blum, M.G.B., 2012. abc: an R package for approximate Bayesian computation (ABC). *Methods Ecol. Evol.* 3, 475–479.
- DeForest Safford, H., 1999. Brazilian Páramos I. An introduction to the physical environment and vegetation of the campos de altitude. *J. Biogeogr.* 26, 693–712.
- de Oliveira, M.A.T., Porsani, J.L., de Lima, G.L., Jeske-Pieruschka, V., Behling, H., 2012. Upper Pleistocene to Holocene peatland evolution in Southern Brazilian highlands as depicted by radar stratigraphy, sedimentology and palynology. *Quat. Res.* 77, 397–407. <https://doi.org/10.1016/j.yqres.2011.12.006>.
- Eisenlohr, P.V., Alves, L.F., Bernacci, L.C., Padgurschi, M.C.G., Torres, R.B., Prata, E.M.B., dos Santos, F.A.M., Assis, M.A., Ramos, E., Rochelle, A.L.C., Martins, F.R., Campos, M.C.R., Pedroni, F., Sanchez, M., Pereira, L.S., Vieira, S.A., Gomes, J.A.M.A., Tamashiro, J.Y., Scaranello, M.A.S., Caron, C.J., Joly, C.A., 2013. Disturbances, elevation, topography and spatial proximity drive vegetation patterns along an altitudinal gradient of a top biodiversity hotspot. *Biodivers. Conserv.* 22, 2767–2783. <https://doi.org/10.1007/s10531-013-0553-x>.
- Elith, J., Kearney, M., Phillips, S., 2010. The art of modelling range-shifting species. *Methods Ecol. Evol.* 1, 330–342.
- Elith, J., Leathwick, J.R., 2009. Species Distribution Models: Ecological Explanation and Prediction Across Space and Time. *Annu. Rev. Ecol. Syst.* <https://doi.org/10.1146/annurev.ecolsys.110308.120159>.
- Elsen, P.R., Tingley, M.W., 2015. Global mountain topography and the fate of montane species under climate change. *Nat. Clim. Chang.* 5, 772. <https://doi.org/10.1038/nclimate2656>.
- Excoffier, L., Foll, M., Petit, R.J., 2009. Genetic Consequences of Range Expansions. *Annu. Rev. Ecol. Syst.* 40, 481–501. <https://doi.org/10.1146/annurev.ecolsys.39.110707.173414>.
- Faircloth, B.C., McCormack, J.E., Crawford, N.G., Harvey, M.G., Brumfield, R.T., Glenn, T.C., 2012. Ultraconserved elements anchor thousands of genetic markers spanning multiple evolutionary timescales. *Syst. Biol.* 61, 717–726. <https://doi.org/10.1093/sysbio/sys004>.
- Farr, T.G., Rosen, P.A., Caro, E., Crippen, R., Duren, R., Hensley, S., Kobrick, M., Paller, M., Rodriguez, E., Roth, L., Seal, D., Shaffer, S., Shimada, J., Umland, J., Werner, M., Oskin, M., Burbank, D., Alsdorf, D., 2007. The Shuttle Radar Topography Mission. *Rev. Geophys.* 45, 1485. <https://doi.org/10.1029/2005RG000183>.
- Fay, J.C., Wu, C.H., 2000. Hitchhiking under positive Darwinian selection. *Genetics* 155, 1405–1413.
- Flantua, S.G.A., Hooghiemstra, H., Grimm, E.C., Behling, H., Bush, M.B., González-Arango, C., Gosling, W.D., Ledru, M.-P., Lozano-García, S., Maldonado, A., Prieto, A.R., Rull, V., Van Boxel, J.H., 2015. Updated site compilation of the Latin American Pollen Database. *Rev. Palaeobot. Palynol.* 223, 104–115. <https://doi.org/10.1016/j.revpalbo.2015.09.008>.
- Flantua, S.G.A., O'Dea, A., Onstein, R.E., Giraldo, C., Hooghiemstra, H., 2019. The flickering connectivity system of the north Andean páramos. *J. Biogeogr.* 41, 1227. <https://doi.org/10.1111/jbi.13607>.
- Françoso, E., Zuntini, A.R., Carnaval, A.C., Arias, M.C., 2016. Comparative phylogeography in the Atlantic forest and Brazilian savannas: pleistocene fluctuations and dispersal shape spatial patterns in two bumblebees. *BMC Evol. Biol.* <https://doi.org/10.1186/s12862-016-0803-0>.
- Freeman, B.G., Class Freeman, A.M., 2014. Rapid upslope shifts in New Guinean birds illustrate strong distributional responses of tropical montane species to global warming. *Proc. Natl. Acad. Sci. U. S. A.* 111, 4490–4494. <https://doi.org/10.1073/pnas.1318190111>.
- Freeman, B.G., Scholer, M.N., Ruiz-Gutierrez, V., Fitzpatrick, J.W., 2018. Climate change causes upslope shifts and mountaintop extirpations in a tropical bird community. *Proc. Natl. Acad. Sci. U. S. A.* 115, 11982–11987. <https://doi.org/10.1073/pnas.1804224115>.
- Frichot, E., Mathieu, F., Trouillon, T., Bouchard, G., François, O., 2014. Fast and efficient estimation of individual ancestry coefficients. *Genetics* 196, 973–983. <https://doi.org/10.1534/genetics.113.160572>.
- Galante, P.J., Alade, B., Muscarella, R., Jansa, S.A., Goodman, S.M., Anderson, R.P., 2018. The challenge of modeling niches and distributions for data-poor species: a comprehensive approach to model complexity. *Ecography* 41, 726–736. <https://doi.org/10.1111/ecog.02909>.
- Gehara, M., Garda, A.A., Werneck, F.P., Oliveira, E.F., da Fonseca, E.M., Camurugi, F., Magalhães, F.de M., Lanna, F.M., Sites Jr, J.W., Marques, R., Silveira-Filho, R., São Pedro, V.A., Colli, G.R., Costa, G.C., Burbrink, F.T., 2017. Estimating synchronous demographic changes across populations using hABC and its application for a herpetological community from northeastern Brazil. *Mol. Ecol.* 26, 4756–4771. <https://doi.org/10.1111/mec.14239>.
- Grabherr, M.G., Haas, B.J., Yassour, M., Levin, J.Z., Thompson, D.A., Amit, I., Adiconis, X., Fan, L., Raychowdhury, R., Zeng, Q., Chen, Z., Mueceli, E., Hacohen, N., Gnirke, A., Rhind, N., di Palma, F., Birren, B.W., Nusbaum, C., Lindblad-Toh, K., Friedman, N., Regev, A., 2011. Full-length transcriptome assembly by RNA-Seq data without a reference genome. *Nat. Biotechnol.* 29, 644–652. <https://doi.org/10.1038/nbt.1883>.
- Graham, C.H., Carnaval, A.C., Cadena, C.D., Zamudio, K.R., Roberts, T.E., Parra, J.L., McCain, C.M., Bowie, R.C.K., Moritz, C., Baines, S.B., Schneider, C.J., VanDerWal, J., Rahbek, C., Kozak, K.H., Sanders, N.J., 2014. The origin and maintenance of montane diversity: integrating evolutionary and ecological processes. *Ecography* 37, 711–719. <https://doi.org/10.1111/ecog.00578>.
- Hackett, S.J., Kimball, R.T., Reddy, S., Bowie, R.C.K., Braun, E.L., Braun, M.J., Chojnowski, J.L., Cox, W.A., Han, K.-L., Harshman, J., Huddleston, C.J., Marks, B.D., Miglia, K.J., Moore, W.S., Sheldon, F.H., Steadman, D.W., Witt, C.C., Yuri, T., 2008. A phylogenomic study of birds reveals their evolutionary history. *Science* 320, 1763–1768. <https://doi.org/10.1126/science.1157704>.
- Hasumi, H., Emori, S., 2004. K-1 coupled gem (mircoc) description K-1 technical report no. 1. Center for climate system research (CCSR, Univ. of Tokyo), National Institute for Environmental Studies (NIES), Frontier Research Center for Global Change (FRGC).
- Hewitt, G.M., 2004. Biodiversity: A climate for colonization. *Heredity*. <https://doi.org/10.1038/sj.hdy.6800365>.
- Hijmans, R.J., Cameron, S.E., Parra, J.L., Jones, P.G., Jarvis, A., 2005. Very high resolution interpolated climate surfaces for global land areas. *Int. J. Climatol.* 25, 1965–1978. <https://doi.org/10.1002/joc.1276>.
- Hijmans, R.J., van Etten, J., 2013. Raster: raster: Geographic data analysis and modeling. R package version 2–3.
- Hudson, R.R., 2002. Generating samples under a Wright-Fisher neutral model of genetic variation. *Bioinformatics* 18, 337–338. <https://doi.org/10.1093/bioinformatics/18.2.337>.
- Janzen, D.H., 1967. Why Mountain Passes are Higher in the Tropics. *Am. Nat.* 101, 233–249. <https://doi.org/10.1086/282487>.
- Kass, J.M., Vilela, B., Aiello-Lammens, M.E., Muscarella, R., Merow, C., Anderson, R.P., 2018. Wallace: A flexible platform for reproducible modeling of species niches and distributions built for community expansion. *Methods Ecol. Evol.* 9, 1151–1156. <https://doi.org/10.1111/2041-210X.12945>.
- Katoh, K., Standley, D.M., 2013. MAFFT multiple sequence alignment software version 7: improvements in performance and usability. *Mol. Biol. Evol.* 30, 772–780. <https://doi.org/10.1093/molbev/mst010>.
- Katzman, S., Kern, A.D., Bejerano, G., Fewell, G., Fulton, L., Wilson, R.K., Haussler, D., 2007. Human genome ultraconserved elements are ultraconserved. *Science* 317 (5840), 915. <https://doi.org/10.1126/science.1142430>.
- Kimball, R.T., Braun, E.L., Barker, F.K., Bowie, R.C.K., Braun, M.J., Chojnowski, J.L., Hackett, S.J., Han, K.-L., Harshman, J., Heimer-Torres, V., Holzner, W., Huddleston, C.J., Marks, B.D., Miglia, K.J., Moore, W.S., Reddy, S., Sheldon, F.H., Smith, J.V., Witt, C.C., Yuri, T., 2009. A well-tested set of primers to amplify regions spread across the avian genome. *Mol. Phylogenet. Evol.* 50, 654–660. <https://doi.org/10.1016/j.ympev.2008.11.018>.
- Kozak, K.H., Wiens, J.J., 2007. Climatic zonation drives latitudinal variation in speciation

- mechanisms. *Proc. Biol. Sci.* 274, 2995–3003. <https://doi.org/10.1098/rspb.2007.1106>.
- Kuhn, M., Wing, J., Weston, S., Williams, A., Keefer, C., Engelhardt, A., Others, 2017. Caret: classification and regression training. 2016. R package version 4.
- La Sorte, F.A., Jetz, W., 2010. Projected range contractions of montane biodiversity under global warming. *Proc. Biol. Sci.* 277, 3401–3410. <https://doi.org/10.1098/rspb.2010.0612>.
- Laurance, W.F., Carolina Useche, D., Shoo, L.P., Herzog, S.K., Kessler, M., Escobar, F., Brehm, G., Axmacher, J.C., Chen, I.-C., Gámez, L.A., Hietz, P., Fiedler, K., Pycrz, T., Wolf, J., Merckord, C.L., Cardelus, C., Marshall, A.R., Ah-Peng, C., Aplet, G.H., del Coro Arizmendi, M., Baker, W.J., Barone, J., Brühl, C.A., Bussmann, R.W., Cicuzza, D., Eilu, G., Favila, M.E., Hemp, A., Hemp, C., Homeier, J., Hurtado, J., Jankowski, J., Kattán, G., Kluge, J., Krömer, T., Lees, D.C., Lehnert, M., Longino, J.T., Lovett, J., Martin, P.H., Patterson, B.D., Pearson, R.G., Peh, K.S.-H., Richardson, B., Richardson, M., Samways, M.J., Senbeta, F., Smith, T.B., Utteridge, T.M.A., Watkins, J.E., Wilson, R., Williams, S.E., Thomas, C.D., 2011. Global warming, elevational ranges and the vulnerability of tropical biota. *Biol. Conserv.* 144, 548–557. <https://doi.org/10.1016/j.biocon.2010.10.010>.
- Ledru, M.-P., Mourguiart, P., Riccomini, C., 2009. Related changes in biodiversity, insolation and climate in the Atlantic rainforest since the last interglacial. *Palaeogeogr. Palaeoclimatol. Palaeoecol.* 271, 140–152. <https://doi.org/10.1016/j.palaeo.2008.10.008>.
- Leite, Y.L.R., Costa, L.P., Loss, A.C., Rocha, R.G., Batalha-Filho, H., Bastos, A.C., Quaresma, V.S., Fagundes, V., Paresque, R., Passamani, M., Pardini, R., 2016. Neotropical forest expansion during the last glacial period challenges refuge hypothesis. *Proc. Natl. Acad. Sci. U. S. A.* 113, 1008–1013. <https://doi.org/10.1073/pnas.1513062113>.
- Li, H., 2011. A statistical framework for SNP calling, mutation discovery, association mapping and population genetical parameter estimation from sequencing data. *Bioinformatics* 27, 2987–2993. <https://doi.org/10.1093/bioinformatics/btr509>.
- Li, H., Durbin, R., 2009. Fast and accurate short read alignment with Burrows-Wheeler transform. *Bioinformatics* 25, 1754–1760. <https://doi.org/10.1093/bioinformatics/btp324>.
- McCormack, J.E., Huang, H., Knowles, L.L., Gillespie, R., Clague, D., 2009. *Sky islands*. *Encyclopedia Islands* 4, 841–843.
- McKenna, A., Hanna, M., Banks, E., Sivachenko, A., Cibulskis, K., Kernytsky, A., Garimella, K., Altshuler, D., Gabriel, S., Daly, M., DePristo, M.A., 2010. The Genome Analysis Toolkit: a MapReduce framework for analyzing next-generation DNA sequencing data. *Genome Res.* 20, 1297–1303. <https://doi.org/10.1101/gr.107524.110>.
- Moritz, C., Patton, J.L., Conroy, C.J., Parra, J.L., White, G.C., Beissinger, S.R., 2008. Impact of a century of climate change on small-mammal communities in Yosemite National Park, USA. *Science* 322, 261–264. <https://doi.org/10.1126/science.1163428>.
- Muscarella, R., Galante, P.J., Soley-Guardia, M., Boria, R.A., Kass, J.M., Uriarte, M., Anderson, R.P., 2014. ENMeval: An R package for conducting spatially independent evaluations and estimating optimal model complexity for Maxent ecological niche models. *Methods Ecol. Evol.* 5, 1198–1205. <https://doi.org/10.1111/2041-210X.12261>.
- Mutke, J., Jacobs, R., Meyers, K., Henning, T., Weigend, M., 2014. Diversity patterns of selected Andean plant groups correspond to topography and habitat dynamics, not orogeny. *Front. Genet.* 5, 351. <https://doi.org/10.3389/fgene.2014.00351>.
- Nosil, P., 2012. *Ecological Speciation*. Oxford University Press.
- Oswald, J.A., Steadman, D.W., 2015. The changing diversity and distribution of dry forest passerine birds in northwestern Peru since the last ice age. *The Auk: Ornithol. Advances*.
- Pavlidis, P., Laurent, S., Stephan, W., 2010. msABC: a modification of Hudson's ms to facilitate multi-locus ABC analysis. *Mol. Ecol. Resour.* 10, 723–727.
- Paz, A., Spanos, Z., Brown, J.L., Lyra, M., Haddad, C., Rodrigues, M., Carnaval, A., 2019. Phylogeography of Atlantic Forest glassfrogs (*Vitreorana*): when geography, climate dynamics and rivers matter. *Heredity* 122, 545–557. <https://doi.org/10.1038/s41437-018-0155-1>.
- Pearson, R.G., 2007. Species' distribution modeling for conservation educators and practitioners. *Synthesis. Am. Museum Nat. History* 50, 54–89.
- Peres, E.A., Sobral-Souza, T., Perez, M.F., Bonatelli, I.A.S., Silva, D.P., Silva, M.J., Solferini, V.N., 2015. Pleistocene niche stability and lineage diversification in the subtropical spider *Araneus omnicolor* (Araneidae). *PLoS ONE* 10, e0121543. <https://doi.org/10.1371/journal.pone.0121543>.
- Peterson, A.T., Townsend Peterson, A., Soberón, J., Pearson, R.G., Anderson, R.P., Martínez-Meyer, E., Nakamura, M., Araújo, M.B., 2011. *Ecological Niches and Geographic Distributions* (MPB-49). <https://doi.org/10.23943/princeton/9780691136868.001.0001>.
- Phillips, S.J., Dudík, M., 2008. Modeling of species distributions with Maxent: new extensions and a comprehensive evaluation. *Ecography* 31, 161–175. <https://doi.org/10.1111/j.0906-7590.2008.5203.x>.
- Pie, M.R., Faircloth, B.C., Ribeiro, L.F., Bornschein, M.R., McCormack, J.E., 2018. Phylogenomics of montane frogs of the Brazilian Atlantic Forest is consistent with isolation in sky islands followed by climatic stability. *Biol. J. Linn. Soc.* <https://doi.org/10.1093/biolinnean/bly093>.
- Polato, N.R., Gill, B.A., Shah, A.A., Gray, M.M., Casner, K.L., Barthelet, A., Messer, P.W., Simmons, M.P., Guayasamin, J.M., Encalada, A.C., Kondratieff, B.C., Flecker, A.S., Thomas, S.A., Ghalambor, C.K., Poff, N.L., Funk, W.C., Zamudio, K.R., 2018. Narrow thermal tolerance and low dispersal drive higher speciation in tropical mountains. *Proc. Natl. Acad. Sci. U. S. A.* 115, 12471–12476. <https://doi.org/10.1073/pnas.1809326115>.
- Portik, D.M., Smith, L.L., Bi, K., 2016. An evaluation of transcriptome-based exon capture for frog phylogenomics across multiple scales of divergence (Class: Amphibia, Order: Anura). *Mol. Ecol. Resour.* 16, 1069–1083.
- Radosavljevic, A., Anderson, R.P., 2014. Making better Maxent models of species distributions: complexity, overfitting and evaluation. *J. Biogeogr.* 41, 629–643.
- Ramírez-Barahona, S., Eguiarte, L.E., 2013. The role of glacial cycles in promoting genetic diversity in the Neotropics: the case of cloud forests during the Last Glacial Maximum. *Ecol. Evol.* 3, 725–738. <https://doi.org/10.1002/ece3.483>.
- Roy, M.S., Da Silva, J.M.C., Arctander, P., García-Moreno, J., Fjeldså, J., 1997. The speciation of South American and African birds in montane regions. In: *Avian Molecular Evolution and Systematics*. Elsevier, pp. 325–343.
- Şekercioğlu, Ç.H., Primack, R.B., Wormworth, J., 2012. The effects of climate change on tropical birds. *Biol. Conserv.* 148, 1–18. <https://doi.org/10.1016/j.biocon.2011.10.019>.
- Shcheglovitova, M., Anderson, R.P., 2013. Estimating optimal complexity for ecological niche models: A jackknife approach for species with small sample sizes. *Ecol. Modell.* 269, 9–17. <https://doi.org/10.1016/j.ecolmodel.2013.08.011>.
- Singarayer, J.S., Valdes, P.J., 2010. High-latitude climate sensitivity to ice-sheet forcing over the last 120 kyr. *Quat. Sci. Rev.* 29, 43–55.
- Smith, Brian T., McCormack, John A., Cuervo, Andrés M., Hickerson, Michael J., Aleixo, Alexandre, Cadena, Carlos D., Pérez-Emán, Jorge, Burney, Curtis W., Xie, Xiaou, Harvey, Michael G., Faircloth, Brant C., Glenn, Travis C., Derryberry, Elizabeth P., Prejean, Jesse, Fields, Samantha, Brumfield, Robb T., et al., 2014. The drivers of tropical speciation. *Nature* 515 (7527), 406–409. <https://doi.org/10.1038/nature13687>.
- Sorte, F.A.L., La Sorte, F.A., Butchart, S.H.M., Jetz, W., Böhning-Gaese, K., 2014. Range-Wide Latitudinal and Elevational Temperature Gradients for the World's Terrestrial Birds: Implications under Global Climate Change. *PLoS ONE*. <https://doi.org/10.1371/journal.pone.0098361>.
- Stotz, D.F., Fitzpatrick, J.W., Parker III, T.A., Moskovits, D.K., 1996. *Neotropical birds: ecology and conservation*. Univ Chicago Press, Chicago.
- Strangas, M.L., Navas, C.A., Rodrigues, M.T., Carnaval, A.C., 2019. Thermophysiology, microclimates, and species distributions of lizards in the mountains of the Brazilian Atlantic Forest. *Ecography*. <https://doi.org/10.1111/ecog.03330>.
- Tajima, F., 1989. Statistical method for testing the neutral mutation hypothesis by DNA polymorphism. *Genetics* 123, 585–595.
- Thom, G., Amaral, F.R., Hickerson, M.J., Aleixo, A., Araujo-Silva, L.E., Ribas, C.C., Choueri, E., Miyaki, C.Y., 2018. Phenotypic and Genetic Structure Support Gene Flow Generating Gene Tree Discordances in an Amazonian Floodplain Endemic Species. *Syst. Biol.* <https://doi.org/10.1093/sysbio/syy004>.
- Tieleman, B.I., Williams, J.B., Buschur, M.E., Brown, C.R., 2003. Phenotypic Variation of Larks Along An Aridity Gradient: Are Desert Birds More Flexible? *Ecology* 84, 1800–1815. [https://doi.org/10.1890/0012-9658\(2003\)084\[1800:PVOLAAJ\]2.0.CO;2](https://doi.org/10.1890/0012-9658(2003)084[1800:PVOLAAJ]2.0.CO;2).
- Watterson, G.A., 1975. On the number of segregating sites in genetical models without recombination. *Theor. Popul. Biol.* 7, 256–276.
- Wiens, J.J., Parra-Olea, G., García-París, M., Wake, D.B., 2007. Phylogenetic history underlies elevational biodiversity patterns in tropical salamanders. *Proc. Royal Soc. B: Biol. Sci.* <https://doi.org/10.1098/rspb.2006.0301>.
- Wright, S., 1950. Genetical structure of populations. *Nature* 166, 247–249. <https://doi.org/10.1038/166247a0>.